JACS
JOURNAL OF THE AMERICAN CHEMICAL SOCIETY

Article

pubs.acs.org/JACS

A Twice-As-Smart Synthetic G-Quartet: PyroTASQ Is Both a Smart Quadruplex Ligand and a Smart Fluorescent Probe

Aurélien Laguerre,[†] Loic Stefan,[†] Manuel Larrouy,[†] David Genest,[†] Jana Novotna,[†,‡] Marc Pirrotta,[†] and David Monchaud*[,†]

[†]Institute of Molecular Chemistry, University of Dijon, ICMUB CNRS UMR6302, 21078 Dijon, France

[‡]Department of Analytical Chemistry, Institute of Chemical Technology, 166 28 Prague, Czech Republic

Supporting Information

ABSTRACT: Recent and unambiguous evidences of the formation of DNA and RNA G-quadruplexes in cells has provided solid support for these structures to be considered as valuable targets in oncology. Beyond this, they have lent further credence to the anticancer strategies relying on small molecules that selectively target these higher-order DNA/RNA architectures, referred to as G-quadruplex ligands. They have also shed bright light on the necessity of designing multitasking ligands, displaying not only enticing quadruplex interacting properties (affinity, structural selectivity) but also additional features that make them usable for detecting quadruplexes in living cells, notably for determining whether, when, and where these structures fold and unfold during the cell cycle and also for better assessing the consequences of their stabilization by external agents. Herein, we report a brand new design of such multitasking ligands, whose structure experiences a quadruplex-promoted conformational switch that triggers not only its quadruplex affinity (i.e., smart ligands, which display high affinity and selectivity for DNA/RNA quadruplexes) but also its fluorescence (i.e., smart probes, which behave as selective light-up fluorescent reporters on the basis of a fluorogenic electron redistribution). The first prototype of such multifunctional ligands, termed PyroTASQ, represents a brand new generation of quadruplex ligands that can be referred to as "twice-as-smart" quadruplex ligands.

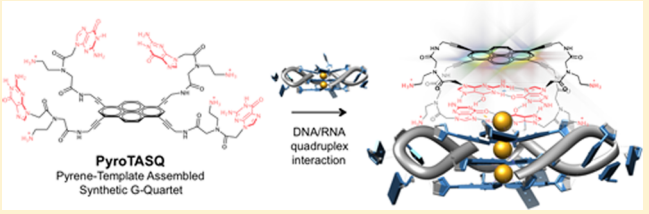

INTRODUCTION

G-quadruplex ligands[1] represent a new class of anticancer agents, the mechanism of which relies on the stabilization of an unusual DNA structure termed G-quadruplex DNA.[2] The quadruplex/ligand assemblies create DNA damages and trigger DNA damage signaling and repair machineries,[3] the so-called DNA damage response (DDR).[4] Most cancer cells being DDR-impaired,[5] or easily chemically impaired (synthetic lethality strategy),[3,6] they are found more sensitive to DNA damaging drugs than their healthy counterparts. G-quadruplex ligands can therefore be considered as a novel class of DNA damaging agents, whose effectiveness rests neither on DNA modifications (i.e., alkylating agents) nor on induction of DNA strand breaks (i.e., antitumor antibiotics), but on the targeting of a noncanonical DNA structures:[7] when stabilized, these higher-order DNA structures pose a serious challenge to DNA transactions, impeding the normal DNA/RNA polymerases processivity, which provides a strong DNA damage signal that leads to the recruitment of the DDR machinery.[3,6,8] Quadruplex ligands are not sequence but structure selective therapeutic agents, therefore displaying a higher, easier to control level of selectivity.

Although indisputable progress has been made over the past years in the use of quadruplex ligands as therapeutic agents,[9] a novel challenge is now taking shape on how to take advantage of the wealth of knowledge gained in the therapeutic arena to design multitasking compounds capable of both interacting with and detecting quadruplex structures, in a cellular context *a fortiori*. Since an increasing number of DNA/RNA sequences able to fold into stable quadruplex structures are currently identified in key regions of both genome and transcriptome,[10] sensing the existence and consequences[11] of quadruplexes in cells is a chemical biology quest of particular significance and strategic relevance. Several successful small-molecule-based approaches have been recently devised, including an outstanding *in cellulo* fluorescent labeling (AlexaFluor) of a ligand (pyridostatin-α) already bound to quadruplexes in living cells,[3] or via the design of fluorescent probes whose spectroscopic properties are turned on upon interaction with quadruplexes, known as light-up probes.[12] The molecular and/or electronic mechanisms underlying the quadruplex-promoted fluorescence enhancement of the light-up dyes are rather ill-defined but mainly fall into two categories, originating either in restriction of intramolecular rotation (RIR), including cyanine (e.g., thiazole orange),[13] benzimidazole (e.g., BPBC),[14] and carbazole derivatives (e.g., BMVC)[15] as well as aggregation-induced emission (AIE) luminogens (e.g., TBE)[16], or in a protection provided by the DNA matrix against water-mediated non-radiative deactivation, including routinely used nucleic acid

Received: June 24, 2014
Published: August 7, 2014

   dx.doi.org/10.1021/ja506331x | J. Am. Chem. Soc. 2014, 136, 12406−12414

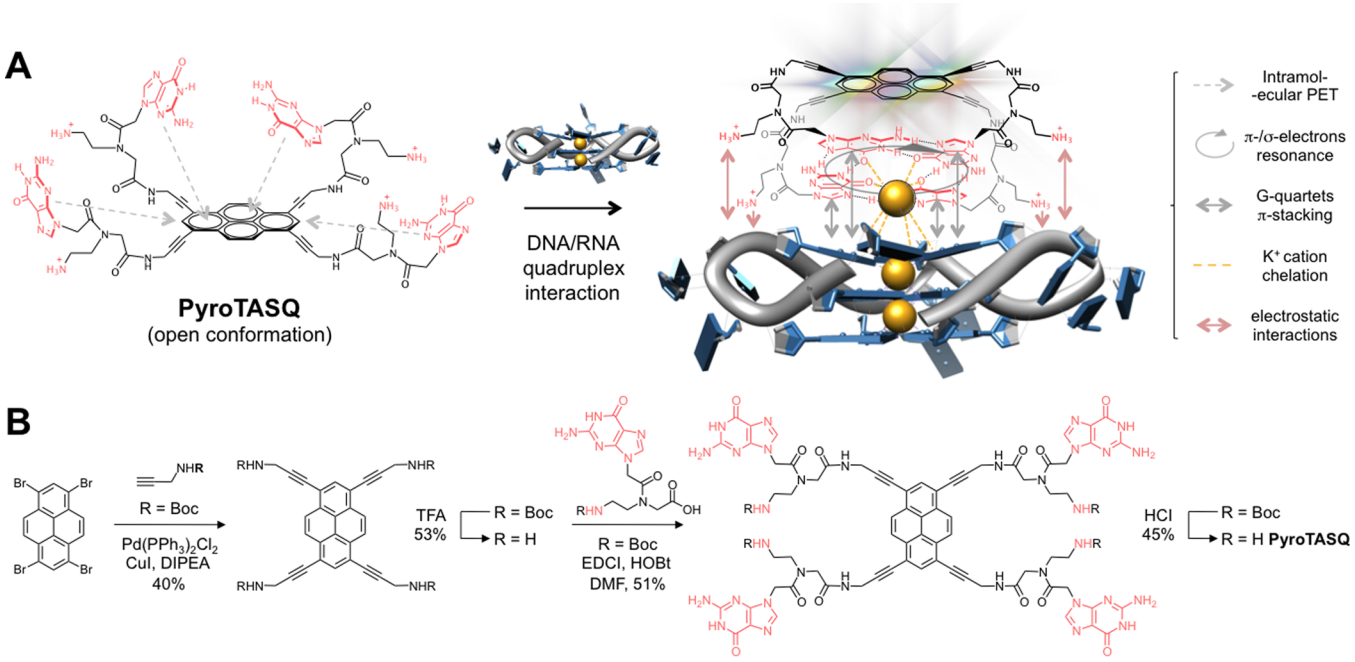

Figure 1. (A) Chemical structure of PyroTASQ and schematic representation of the "twice-as-smart ligand" principle: under its open conformation (left panel), the fluorescence of the pyrene template is quenched by the proximal guanines via an intramolecular photoinduced electron transfer (iPET, gray dashed arrows); upon interaction with a quadruplex, PyroTASQ folds into its closed conformation (right panel) on the basis of a bioinspired binding mode driven by quartet self-association (gray arrows) and promoted by cation chelation (yellow dashed lines) and electrostatic interactions (pink arrows); the formation of the intramolecular quartet leads to a redistribution of the guanine electrons (round gray arrow) that relieves the pyrene from the iPET electronic restraint, causing its fluorescence to be restored. (B) Four-step chemical synthesis of PyroTASQ (see Supporting Information for full details).

staining agents (e.g., ethidium bromide)[17] and porphyrins (e.g., NMM)[18] as well as metal complexes (e.g., Pt(II),[19] Ru(II),[20] and Zn(II)[21] complexes)[22]. To date, only a few studies have been devoted to devising alternative light-up strategies, including an elegant oligonucleotide-templated reaction (OTR) reported by Ladame and co-workers;[23] herein, we report a novel approach that exploits a fluorogenic electron redistribution of synthetic G-quartets that concomitantly act as smart quadruplex ligand and smart fluorescent probe, thereby making them a brand new generation of what can be referred to as "twice-as-smart" quadruplex ligands.

RESULTS AND DISCUSSION

Definition of a Smart Quadruplex Ligand. Most of the G-quadruplex ligands reported so far directly originate from fine structural tunings of the duplex-DNA intercalator pool.[9,24] This approach is somewhat counterintuitive since the interaction with duplex-DNA is the major unwanted event for a compound to be a promising ligand. Structural tuning, like expanding the aromatic core or multiplying the side-arms, was astutely implemented to dampen interactions with duplex binding sites (base-pairs, grooves) to the benefit of the quadruplex one (external G-quartet);[25] but in most cases the selectivity level reached remains perfectible, especially since an overwhelming majority of DNA is present under its duplex form in cell's nuclei. We recently reported on an alternative way to design G-quadruplex ligands, whose quadruplex selectivity is being leveraged through a quadruplex-promoted conformational switch of its structure, thereby ensuring enticing levels of selectivity.[26] Inspired by the strategy implemented by the nature itself to make quadruplex structures so stable, i.e., the stacking of G-quartets atop each other with the concomitant neutralization of the electrostatic repulsion of inwardly pointing guanine oxygens by physiologically relevant cations, chiefly potassium, we used synthetic G-quartets as quadruplex ligands. The logic behind using template-assembled synthetic G-quartets (TASQ)[27] as ligands was two-fold: on one hand, to demonstrate that bioinspired ligands are valuable candidates, acting through a like-likes-like approach,[28] i.e., the recognition and self-assembly of G-quartets, native and synthetic; on the other hand, to exploit this unique self-assembly to make the ligand adopt the suited conformation upon interaction with its target only, the exact definition of a smart ligand.[26] The previously reported prototype, ^{PNA}DOTASQ, was the very first, thoroughly satisfactory example of a smart quadruplex ligand, both in terms of affinity and selectivity. The in depth study of its quadruplex-interacting properties enabled us to firmly demonstrate the DNA/RNA-quadruplex-promoted conformational switch between its open (i.e., unassociated guanines) and closed (i.e., intramolecular quartet fold) conformations, which governs its efficiency and makes it a smart ligand.[26,29]

Definition of a Twice-As-Smart Quadruplex Ligand. To make a further leap along the road toward innovative, multitasking quadruplex ligands, new prototypes of smart G-quadruplex ligand must display not only enticing DNA/RNA quadruplex recognition performances but also quite unique fluorescence properties, notably to make them quadruplex-selective smart fluorescence probes. The aforementioned DNA/RNA-promoted conformational switch of the ligand structure makes it prone to interact with quadruplexes through a bioinspired association relying on the laying of synthetic quartets (ligands) atop native quartets (the privileged small-molecule binding site of a quadruplex architecture). Interestingly, this quartet−quartet interaction is known for leading to a

dx.doi.org/10.1021/ja506331x | J. Am. Chem. Soc. 2014, 136, 12406−12414

Table 1. Oligonucleotides Used in This Study

status	nature	name	sequence
labeled	DNA	F21T	FAM-d[$^{5'}$GGGTTAGGGTTAGGGTTAGGG$^{3'}$]-TAMRA
		F-myc-T	FAM-d[$^{5'}$GAGGGTGGGGAGGGTGGGGAAG$^{3'}$]-TAMRA
		F-kit-T	FAM-d[$^{5'}$CGGGCGGGCGCGAGGGAGGGG$^{3'}$]-TAMRA
		F-duplex-T	FAM-d[$^{5'}$TATAGCTATATTTTTTTATAGCTATA$^{3'}$]-TAMRA
	RNA	L-TERRA	FAM-r[$^{5'}$GGGUUAGGGUUAGGGUUAGGG$^{3'}$]-TAMRA
		L-TRF2	FAM-r[$^{5'}$CGGGAGGGCGGGGAGGGC$^{3'}$]-TAMRA
		L-VEGF	FAM-r[$^{5'}$GGAGGAGGGGAGGAGGA$^{3'}$]-TAMRA
unlabeled	DNA	22AG	d[$^{5'}$AGGGTTAGGGTTAGGGTTAGGG$^{3'}$]
		c-myc	d[$^{5'}$GAGGGTGGGGAGGGTGGGGAAG$^{3'}$]
		c-kit	d[$^{5'}$CGGGCGGGCGCGAGGGAGGGG$^{3'}$]
		SRC	d[$^{5'}$GGGAGGGAGGGCTGGGGG$^{3'}$]
		TG5T	strands 1−4: d[$^{5'}$TGGGGGT$^{3'}$]
		$d[T_2AG_3T]_4$	strands 1−4: d[$^{5'}$TTAGGGT$^{3'}$]
		ds17	strand 1: d[$^{5'}$CCAGTTCGTAGTAACCC$^{3'}$]
			strand 2: d[$^{5'}$GGGTTACTACGAACTGG$^{3'}$]
		ds26	strand 1: d[$^{5'}$CAATCGGATCGAATTCGATCCGATTG$^{3'}$]
			strand 2: d[$^{5'}$GTTAGCCTAGCTTAAGCTAGGCTAAC$^{3'}$]
	RNA	TERRA	r[$^{5'}$GGGUUAGGGUUAGGGUUAGGG$^{3'}$]
		TRF2	r[$^{5'}$CGGGAGGGCGGGGAGGGC$^{3'}$]
		VEGF	r[$^{5'}$GGAGGAGGGGAGGAGGA$^{3'}$]
		UG5U	strands 1−4: r[$^{5'}$UGGGGGU$^{3'}$]

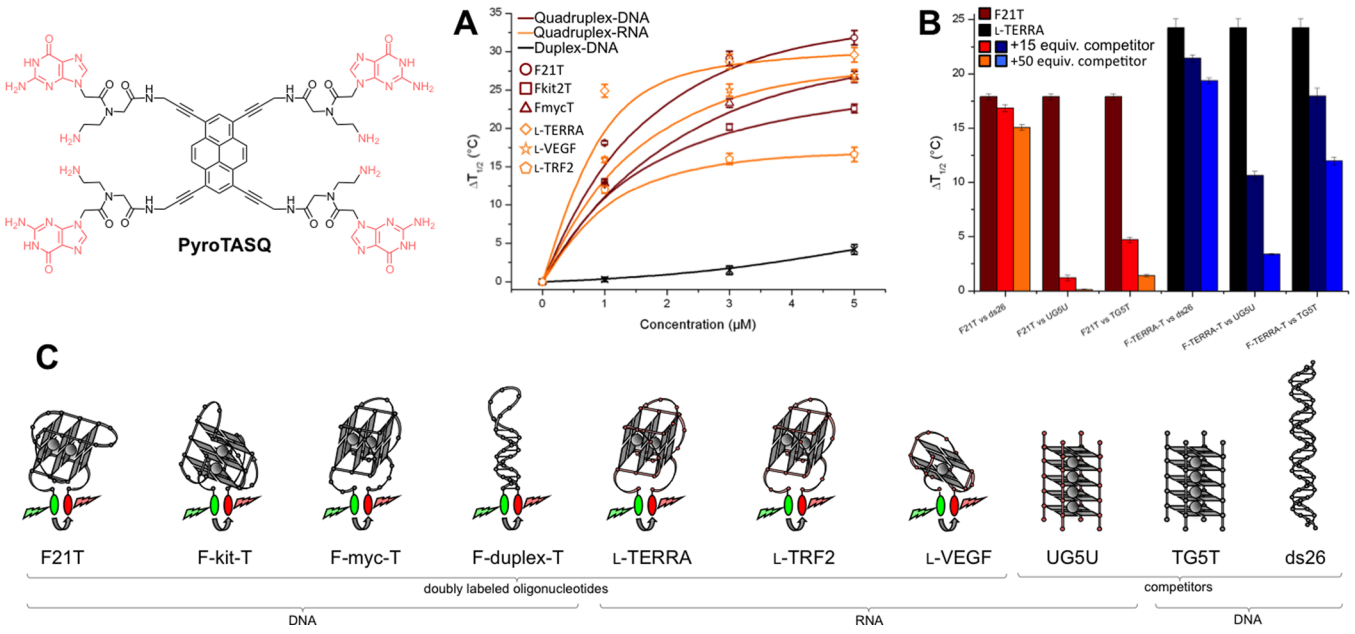

Figure 2. (A) FRET-melting results of experiments carried out with quadruplex-DNA (F21T, F-kit-T and F-myc-T, 0.2 μM, brown lines), quadruplex-RNA (L-TERRA, L-VEGF and L-TRF2, 0.2 μM, orange lines), or duplex-DNA (F-duplex-T, 0.2 μM, black line) with increasing amounts (0−5 μM) of PyroTASQ. (B) Competitive FRET-melting results of experiments carried out with quadruplex-DNA (F21T, 0.2 μM, brown bars) or quadruplex-RNA (L-TERRA, 0.2 μM, black bars) PyroTASQ (1 μM) and increasing amounts (3 and 10 μM) of unlabeled competitors (ds26, TG5T or UG5U, orange and blue bars). (C) Schematic representation of the oligonucleotides used in the FRET-melting experiments.

redistribution of the synthetic guanine electrons that could be exploited to fluorescently sense the formation of the intramolecular quartet, i.e., the ligand/quadruplex interaction. Thus, through a judicious choice of the template used to assemble intramolecularly the four guanines, new TASQ may become attractive light-up probes, and beyond this, the very first prototypes of a twice-as-smart quadruplex ligand, being concomitantly a smart ligand and a smart fluorescent probe, whose optical properties are governed by an original electronic mechanism.

To this end, novel TASQ templates have been selected on the basis of strict specifications: their fluorescence properties must be interesting enough for the TASQ to be valuable fluorescent probes, but effectively quenched by free proximal guanines to define the off-state of the probe; sensitive enough to sense the electronic rearrangement of the guanines folding into an intramolecular quartet, but not too much not to be deactivated by solvent effects only; their chemical access must be not only convenient, i.e., straightforwardly synthesized and modified, but also modular since four guanine arms must be inserted; etc. For all these reasons, we turned our attention on

dx.doi.org/10.1021/ja506331x | J. Am. Chem. Soc. 2014, 136, 12406−12414

polycyclic aromatic hydrocarbons (PAH, herein pyrene). The choice of a pyrene template might appear unwise at first glance: pyrene is indeed known to be poorly water-soluble and to display fluorescence properties that are only limitedly compatible with biological applications; however, the pyrene fluorescence properties are known to be readily and quite efficiently quenched by guanines.[30]

The novel synthetic G-quartet reported herein is named PyroTASQ, for pyrene template-assembled synthetic G-quartet (Figure 1). The way PyroTASQ was designed enabled us to tackle the aforementioned drawbacks and turn them into advantages: (i) The water solubility problem was readily solved by the nature of the guanine side arms appended around the PAH template, i.e., the cationic peptidic nucleic acid (PNA) guanine monomer (^{PNA}G) that was successfully employed for ^{PNA}DOTASQ:[26] four of these arms provide high water solubility (PyroTASQ is soluble at 10 mM in water) in addition to being responsible of the quadruplex-promoted affinity-triggering conformational switch of the resulting TASQ. (ii) The bioapplication adequacy, mainly the spectroscopic properties, was subsequently dealt with, following a strategy classically implemented to displace the pyrene absorbance toward higher wavelengths, notably higher than that of biomolecules including DNA, i.e., to decrease its electron density through the connection of electron-withdrawing groups;[31] herein, the four ^{PNA}G were thus grafted via a challenging quadruple palladium-catalyzed Sonogashira–Heck–Cassar alkynylation reaction (Figure 1B and Supporting Information)[32] to make pyrene surrounded by four triple bonds that greatly expand its π-electron conjugation, thereby making it less electron-rich (*vide infra*). (iii) Finally, and as further discussed below, the presence within the same scaffold of a pyrene and four guanines indeed results in a completely quenched PAH fluorescence via an intramolecular photoinduced electron transfer (iPET) mechanism (Figure 1A);[33] this effective quench is beneficial herein since it defines the off-state of the fluorescence probe.

Quadruplex-Interacting Properties of PyroTASQ. Before investigating the spectroscopic properties of both free and quadruplex-bound PyroTASQ, its DNA/RNA quadruplex-recognition properties were assessed. To this end, fluorescence resonance energy transfer (FRET)-melting assays[34] were implemented with PyroTASQ against a panel of biologically relevant doubly labeled quadruplex-forming sequences, including F21T, F-myc-T and F-kit-T, which are DNA sequences found in the human telomeres[35] and in the promoter region of myc and kit genes,[36] respectively (Table 1), and L-TERRA, L-TRF2, and L-VEGF, which are RNA sequences found in telomeric transcripts[37] and in the untranslated region (5′-UTR) of mRNA of the telomeric repeat binding factor 2 (TRF2) and vascular endothelial growth factor (VEGF) genes,[38] respectively (Table 1). As seen in Figure 2A, PyroTASQ stabilizes quadruplexes efficiently whatever their nature, with $\Delta T_{1/2}$ values comprised between 12.8–18.1 °C and 12.0–24.9 °C with DNA and RNA quadruplexes, respectively, at 1 μM concentration. PyroTASQ is thus a more efficient ligand than ^{PNA}DOTASQ, with $\Delta T_{1/2}$ values between 12.3–15.2 °C and 10.1–21.2 °C for DNA and RNA quadruplexes, respectively. PyroTASQ is also exquisitely quadruplex vs duplex selective, as demonstrated by the low F-duplex-T stabilization, 4 °C at 5 μM concentration (Figure 2A). This was further assessed via competitive FRET-melting experiments carried out with F21T in the presence of 0, 15, and 50 mol equiv of unlabeled 26-bp duplex-DNA ds26 (Table 1): as seen in Figure 2B, the F21T stabilization is maintained at 94 and 84% in the presence of 15 and 50 mol equiv ds26, respectively, thereby highlighting the excellent selectivity and so the interest of TASQ-based quadruplex ligands. Of note, a similar series of experiments carried out with the control compound PyroNH$_2$, which is a cationic and water-soluble pyrene derivative devoid of guanine arms (see Supporting Information) clearly highlights that the guanines side arms are entirely accountable for the aforementioned excellent properties of PyroTASQ.

A second series of competitive FRET-melting experiments was carried out with F21T in the presence of 0, 15, and 50 mol equiv of unlabeled tetramolecular DNA/RNA quadruplexes, i.e., devoid of loops and thus exhibiting two highly accessible external G-quartets, to gain insights into the actual binding site of PyroTASQ. The F21T stabilization is greatly affected by the presence of 15 and 50 mol equiv TG5T ($d[TG_5T]_4$, with 26 and 8% remaining stabilization, respectively) but, interestingly, is even more affected by its RNA counterpart, termed UG5U ($r[UG_5U]_4$, with 7 and 1% remaining stabilization, respectively). This indicates not only that PyroTASQ is highly sensitive to an excess of accessible G-quartet, and so that the external quartet of a quadruplex is its privileged binding site, but also that it might interact with quadruplex-RNA more efficiently. To further investigate this, a final series of competitive FRET-melting experiments was undertaken with L-TERRA in the presence of 0, 15, and 50 mol equiv of ds26, TG5T, and UG5U (Table 1). Results seen in Figure 2B can be interpreted as follows: (i) the ds26 competition confirms the excellent quadruplex-vs-duplex selectivity of PyroTASQ, the L-TERRA stabilization being maintained at 88 and 80% in the presence of 15 and 50 mol equiv ds26, respectively; (ii) the L-TERRA stabilization is limitedly affected by an excess of TG5T, being maintained at 74 and 49% in the presence of 15 and 50 mol equiv TG5T, respectively, implying that, reminiscently of what has been observed with ^{PNA}DOTASQ,[29] PyroTASQ elicits a preferential affinity for RNA-quadruplexes; and finally (iii) the strong UG5U competition (43 and 14% of L-TERRA stabilization in the presence of 15 and 50 mol equiv UG5U) again demonstrates the sensitivity of PyroTASQ to the presence of competitive G-quartets. Altogether, these results clearly indicate that PyroTASQ is an excellent DNA/RNA quadruplex ligand, which additionally elicits an interesting preferential affinity for RNA quadruplexes. The origins of this preferential affinity remain at present unclear: in light of the previously reported examples,[29,39,40] we can postulate that selective interactions may take place between the 2′-OH group of the RNA sugar (i.e. absent in the corresponding DNA quadruplex) and the amine side arms of PyroTASQ; alternatively, the nature of the sugar itself can make the RNA G-quartet more sterically accessible than its DNA counterpart. However, in any case, efforts have to be massively invested to decipher the actual origins of this RNA-versus-DNA preference.

Principle of the Fluorogenic Electron Redistribution That Makes PyroTASQ A Twice-As-Smart Quadruplex Ligand. The electronic behavior of guanines and guanine/pyrene partners strongly depends on their coordination state, being either free or involved in a quartet: when free (TASQ open conformation), the high electron density of guanines results in an PET phenomenon known to quench the pyrene fluorescence,[30] as firmly demonstrated through fluorescence investigations carried out with water-soluble pyrene and guanine derivatives (PyroNH$_2$ and GMP, see Supporting

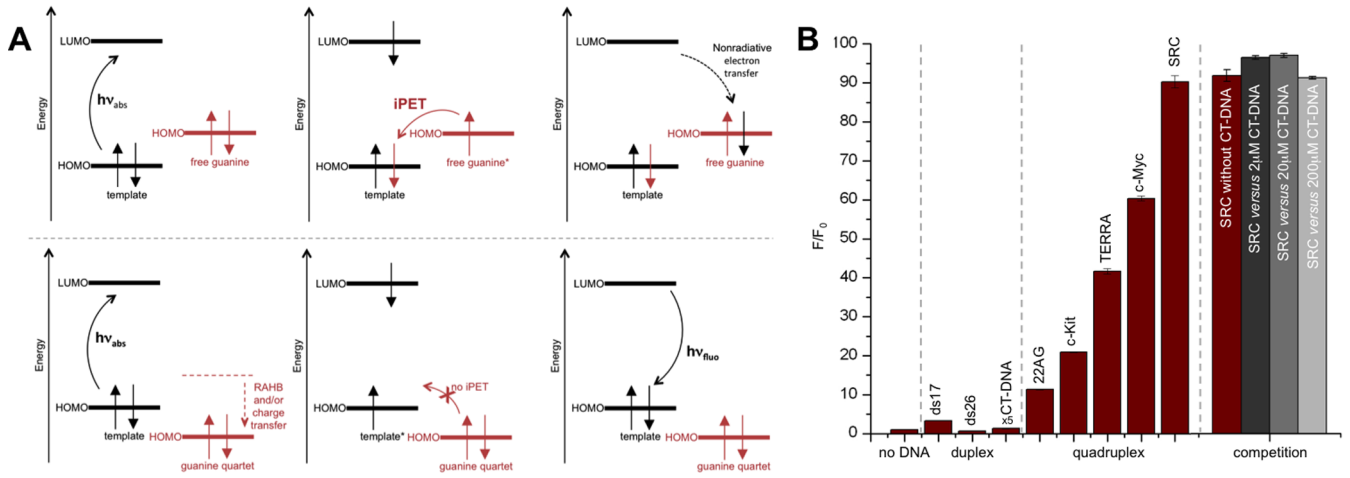

Figure 3. (A) Molecular orbital theory that underlies the twice-as-smart ligand principle. (B) Fluorescence studies (λ_{ex} = 420 nm, λ_{em} = 445 ± 5 nm depending on the DNA) of PyroTASQ (2 μM) alone ("no DNA" bar) or in presence (4 μM) of duplexes (ds17, ds26, and CT-DNA) or quadruplexes (22AG, c-kit, TERRA, c-myc, and SRC). Competitive fluorescence experiments carried out with PyroTASQ (2 μM), a quadruplex (SRC, 4 μM) and increasing amounts of a duplex (CT-DNA, 2−200 μM). Experiments are carried out in 10 mM lithium cacodylate buffer (pH 7.2) + 90 mM LiCl/10 mM KCl at room temperature, after a 15 min equilibration step.

Information). The iPET is made possible by an energy level of the highest occupied molecular orbital (HOMO) of the free guanine in between the HOMO and lowest unoccupied molecular orbital (LUMO) of the pyrene (Figure 3A).[33] Conversely, the G-quartet formation (TASQ closed conformation) triggers a redistribution of the guanine electron cloud: indeed, when a guanine becomes involved in a G-quartet, the redistribution of its electron density is a well-documented phenomenon referred to as resonance-assisted hydrogen bonding (RAHB);[41] G-quartet stability is assumed to result from an electronic redistribution ascribed to an interplay between H-bond formation and delocalization of the guanine π-electrons (resonance). RAHB has been recently challenged by a novel theory (the "charge separation" theory)[42] involving not π- but σ-electrons, explaining the stability of a G-quartet by a synergy between H-bond formation and donor (N and O lone-pairs)/acceptor (N−H antibonding) orbitals interactions in the σ-electron system. Although different in nature, both theories agree with a redistribution of the guanine electron density via the formation of a G-quartet; this, combined with the π-stacking interactions between native (quadruplex) and synthetic (ligand) G-quartets, promoted and strengthened by the intercalating cations (K^+), results in a quartet HOMO lower in energy than the free guanine HOMO (Figure 3A). Our hypothesis is thus that the guanine self-assembly makes the quartet HOMO lower in energy than that of the pyrene, thereby weakening or annihilating the iPET phenomenon and consequently restoring the template fluorescence. Pyrene fluorescence might thus be turned on when the TASQ folds into its closed conformation upon interaction with its target, the exact definition of a smart probe.

To demonstrate that PyroTASQ may act as a quadruplex-selective fluorescent smart probe, its spectroscopic properties were assessed: quite satisfyingly, the highest absorbance maximum of PyroTASQ (434 nm in water, versus 336 nm for naked pyrene) makes it suited for biophysical studies with DNA. A series of fluorescent titrations was thus undertaken with PyroTASQ alone or against a panel of biologically relevant oligonucleotides (see Figure 3B and Supporting Information), including both synthetic (ds17, ds26) and natural duplexes (calf-thymus DNA, or CT-DNA) and quadruplexes that are the unlabeled counterparts of the FRET-melting oligonucleotides, namely 22AG, c-kit, c-myc, TERRA and SRC[3] (Table 1). The results of the fluorescence experiments (λ_{ex} = 420 nm, Figure 3B and Supporting Information) show that PyroTASQ fluorescence is almost totally quenched in solution, thereby lending strong support to the hypothesis according to which iPET prevails when the ligand is in its open conformation (*vide infra*). In stark contrast, DNA makes PyroTASQ fluorescent, in a very interesting structure-dependent manner, from poor upon interaction with duplexes up to ∼3-fold enhancement only to very strong enhancements with quadruplexes up to ∼90-fold. These results thus infer that the PyroTASQ fluorescence is indeed driven by the RAHB/charge separation phenomenon, which itself depends on the quadruplex-promoted closed conformation of the ligand.

Comparisons of fluorescence responses between duplexes and quadruplexes clearly enlighten that PyroTASQ is a quadruplex-selective fluorescent probes; this certainly originates in the fact that duplex matrices fail to promote the intramolecular quartet fold of the ligand. This was subsequently confirmed by competitive titrations, in which the fluorescence of PyroTASQ was assessed in the concomitant presence of duplex and quadruplex: the quadruplex (SRC)-triggered fluorescence is not affected by a large excess of duplex, neither CT-DNA (up to 200 μM, Figure 3B) nor ds26 (see Supporting Information). These results make PyroTASQ an enticingly promising probe, notably for in cell investigations. Further analyses of the results depicted in Figure 3B also highlight better enhancements with quadruplexes displaying highly accessible G-quartets, i.e., devoid of adjacent diagonal or lateral loops, whose structure is usually referred to as "parallel" (i.e., TERRA, c-myc, and SRC), thus belonging to group I according to the classification of Spada, Randazzo, and Webba da Silva,[43] than with quadruplexes from groups II and III (∼11- and ∼20-fold increase with 22AG and c-kit, respectively). We can thus postulate that PyroTASQ acts as a highly sensitive structure-selective fluorescent probe. The differences of fluorescence response within the quadruplex series might result from two concomitant but counteracting effects: (i) The positive effect of

dx.doi.org/10.1021/ja506331x | J. Am. Chem. Soc. 2014, 136, 12406−12414

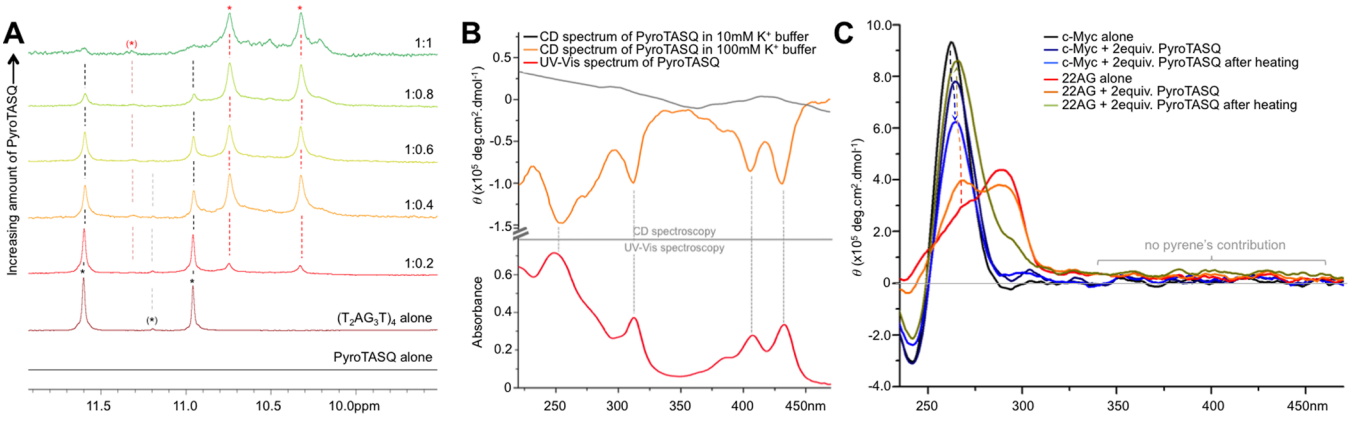

Figure 4. (A) Part (9−12 ppm) of ^{1}H NMR spectra (600 MHz, 10 mM lithium cacodylate buffer (pH 7.2) + 90 mM LiCl/10 mM KCl, 10% D_2O) of PyroTASQ alone (224 μM, black spectrum), the quadruplex-DNA d[$(T_2AG_3T)_4$] alone (224 μM, brown spectrum) or in the presence of increasing amounts (46−224 μM) of PyroTASQ (from red to green spectra). Black stars indicate the quadruplex alone, red stars the quadruplex/ligand assembly. (B) CD experiments carried out with PyroTASQ (30 μM) in 10 mM lithium cacodylate buffer (pH 7.2) + 90 mM LiCl/10 mM KCl (black line) or +100 mM KCl (orange line). Red line corresponds to the UV−vis spectrum of PyroTASQ (10 μM) in 10 mM lithium cacodylate buffer (pH 7.2) + 90 mM LiCl/10 mM KCl. (C) CD spectra of quadruplexes (c-myc or 22AG, black and red line, respectively), alone (2 μM) or in the presence of PyroTASQ (4 μM), before (dark blue and orange lines) or after a thermal annealing step (light blue or green lines), in 10 mM lithium cacodylate buffer (pH 7.2) + 90 mM LiCl/10 mM KCl, 50% CH_3CN.

the external G-quartet accessibility: the better accessibility of the quartet of group I quadruplexes (TERRA, c-myc and SRC) implies better π-stacking interactions with the intramolecular synthetic G-quartet (iSQ), thereby resulting in a better quartet planarity and intermolecular π-stacking interactions, i.e., a more efficient dequenching of the pyrene template. (ii) The negative effect of the external G-quartet steric environment: quadruplexes from group I are characterized by loop-free external G-quartets, while that of groups II and III display external quartets surrounded by loops;[43] therefore, loop nucleobases might be close enough to the pyrene template of the bound PyroTASQ to hamper to some extent its overall fluorescence via an intermolecular PET phenomenon, thereby resulting in a lower overall fluorescence response of groups II and III quadruplexes (i.e., 22AG and c-kit). When combined, these two effects thus make PyroTASQ a highly sensitive structure-selective fluorescent light-up probe.

The Origins of the Spectroscopic Properties of PyroTASQ. To gain insights into the actual twice-as-smart nature of PyroTASQ (smart ligand, smart probe), notably to decipher the electronic redistribution responsible for the quench/dequench of its template fluorescence, a series of nuclear magnetic resonance (NMR)[44] and circular dichroism (CD)[43] experiments were undertaken. We first tackled the demonstration of the PyroTASQ smart ligand nature: the efficient PyroTASQ/quadruplex interactions enlightened by the aforedescribed FRET-melting experiments certainly originate in a stable quadruplex-promoted closed TASQ fold. This prompted us to investigate whether this conformation can be visualized by NMR spectroscopy. Several NMR experiments were performed: (i) with PyroTASQ alone (black line, Figure 4A) and (ii) with a quadruplex alone (brown line, Figure 4A): herein, a tetramolecular quadruplex model routinely used for NMR investigations d[$T_2AG_3T]_4$ was selected for the simplicity of its NMR spectrum in the 10−12 ppm region corresponding to the "imino" protons characteristics of G-quartets: one G-quartet gives rise to one signal, thus implying that the quadruplex structure is herein characterized by three signals only at 10.96, 11.19, and 11.61 ppm (black stars, Figure 4A).[45] Reminiscent of what we already reported during the ^{PNA}DOTASQ study,[26] the imino proton that corresponds to the central G-quartet (at 11.19 ppm) is herein barely visible, presumably because of its location—buried within the quadruplex core—which makes it more shielded from the deuterated environment than the imino protons belonging to the external G-quartets.[46] (iii) Finally, with the quadruplex and increasing amounts of PyroTASQ (from 0 to 1 mol equiv, from red to green curves, Figure 4A). Results seen in Figure 4A not only indicate that PyroTASQ alone is indeed in its open conformation when free in solution (no signals found in the 10−12 ppm region, black line) but also further bolster the strong ligand/quadruplex interaction since the signals of the DNA alone (black stars) almost totally disappear to the benefit of the ligand/quadruplex complex (only the signals corresponding to the two external G-quartets are clearly identifiable, at 10.33 and 10.75 ppm, red stars, Figure 4A) at 1:1 ratio (versus 2:1 with ^{PNA}DOTASQ).[26] However, the PyroTASQ conformational switch can be visualized via a rather ill-defined signal only in the region of the iSQ at 11.3 ppm (bracketed red star): this is not unexpected since line-broadening effects are classically observed during NMR titrations of ligand/DNA interactions;[47] here the pyrene template behaves as a G-quartet ligand for its own quartet (via intramolecular π-stacking interactions), thereby enlightening that both aromatic moieties of PyroTASQ are electronically correlated (*vide infra*). The NMR results thus provide insights into the iSQ formation and also into the actual PyroTASQ binding mode, since the pyrene affects the signals of its own G-quartet only and not that of the quadruplex, implying that it does not contact with them directly, thus supporting the synthetic quartet/native quartet interaction as the privileged binding mode. To further investigate the intramolecular electronic correlation within the PyroTASQ structure, we implemented CD investigations, inspired by recent CD studies of isolated G-quartet/ligand interactions.[48] As seen in Figure 4B, the lack of any significant CD signature (black line) confirms that PyroTASQ free in solution does not adopt its closed conformation under standard conditions (10 mM lithium cacodylate buffer pH 7.2 + 90 mM LiCl and 10 mM KCl). Interestingly, increasing the buffer K^+ content (10 mM lithium cacodylate pH 7.2 + 100 mM KCl) triggers its

dx.doi.org/10.1021/ja506331x | J. Am. Chem. Soc. 2014, 136, 12406−12414

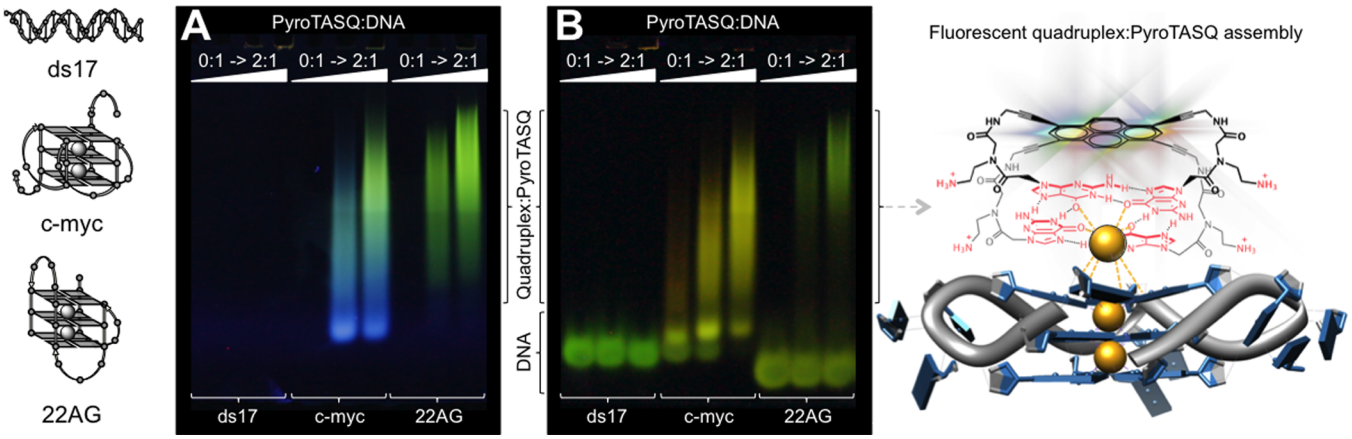

Figure 5. Fluorescence analysis (λ_{ex} = 254 nm) of a polyacrylamide gel (6%, 1 × TBE, pH 8.3) with DNA (duplex (ds17) and quadruplexes (c-myc and 22AG), 50 μM, 5 μL) and increasing amounts of PyroTASQ (from 0 to 100 μM) after migration (50 V, 2 h, 4 °C). Pictures are taken directly after migration (A) and after a poststaining step with SYBR Safe (B).

conformational switch, as demonstrated by the CD signature (orange line) that perfectly mirrors the UV−vis spectrum (red line). Reminiscent of what has been reported by Sherman et al.,[48] this CD signal is comprised of both guanine quartet (220−300 nm) and pyrene (350−450 nm) contributions, indicating that both partners are indeed electronically connected. This signal, which could be referred to as induced CD (iCD) signal given the achiral nature of the compound, thus highlights that PyroTASQ might adopt a closed conformation alone in solution but marginally (low-intensity CD signals) and under precise experimental conditions only, i.e., at elevated concentrations of both PyroTASQ and potassium; indeed, as depicted in the Supporting Information, in potassium-rich conditions (100 mM KCl), a concentration of at least 20 μM of PyroTASQ is required to trigger a significant CD signature, thereby indicating that a higher-order self-assembly of PyroTASQ certainly provides a basis for this dichroic behavior; contrarily, at low potassium level (10 mM KCl), even high concentrations of PyroTASQ do not provide any reliable CD signatures (further bolstered by the NMR spectrum of PyroTASQ alone, Figure 4A). Given that biophysical experiments are routinely carried out with PyroTASQ in the low micromolar range, this series of results clearly indicates that while PyroTASQ may artificially adopt its closed conformation (high PyroTASQ and K^+ concentrations), it remains overwhelmingly under its open conformation under standard experimental conditions. A series of CD titrations were subsequently performed with PyroTASQ (4 μM) in the presence of quadruplexes (both 22AG and c-Myc, 2 μM), in conditions recently described by Chaires et al. as favorable for structural changes (potassium cacodylate buffer/acetonitrile 50% v/v):[49] as seen in Figure 4C, the ligand influences the topologies of the two studied quadruplex structures (with a greater impact on group II than on group I quadruplexes, i.e., 22AG and c-myc, respectively), in both kinetic and thermodynamic conditions, i.e., without or with a thermal annealing step, thus showing again that strong interactions take place between PyroTASQ and quadruplexes (corresponding results in acetonitrile-free conditions are reported in the Supporting Information). However, no iCD signals corresponding to the pyrene template (350−450 nm) are observed, indicating that the electronic connection between the pyrene and iSQ is disrupted when the ligand is interacting with its target: this demonstrates that the ligand stacking atop quadruplexes diverts the guanine electrons from iPET (turn off contribution) to both quartet-promoted electron resonance and intermolecular quartet/quartet π-stacking interactions (turn on contributions), thereby making the quadruplex/ligand assembly a trigger event for the PyroTASQ fluorescence to be turned on in a highly specific manner (i.e., a quadruplex-specific smart fluorescent probes).

PyroTASQ Enables an Easy and Selective Visualization of Quadruplexes. To exploit the fluorescence properties of PyroTASQ, its ability to enlighten quadruplex was assessed via a polyacrylamide gel electrophoresis (PAGE) analysis, a technique known to be quite challenging for investigating noncovalent interactions. PAGE is indeed routinely implemented with DNA alone (for purification or conformational analysis purposes)[50] or upon interaction with covalent DNA linkers, chiefly platinum complexes;[51] conversely, the noncovalent DNA/small-molecule assemblies, especially those driven by external π-stacking interactions only like quadruplex/ligand complexes, are not ideally suited for PAGE analysis since they readily dissociate during the electric field-directed migration on a gel phase (quadruplex fluorescent markers, like ThT[52] or distyrylpyridinium[53] dyes, are routinely used after the gel migration, i.e., as poststaining agents). As seen in Figure 5A, the electrophoretic mobility shift assay (EMSA, 1 × TBE, pH 8.3, 50 V, 4 °C, 2 h) performed with DNA (50 μM), i.e., one duplex (ds17) and two quadruplexes (c-myc and 22AG), and increasing amounts of PyroTASQ (0:1, 1:1 and 2:1 ligand:DNA ratio) unequivocally demonstrates the interest of PyroTASQ as a fluorescent probe: only its complexes with quadruplex are fluorescent, with a slower migration as compared to quadruplex alone, due to its lower overall charge and higher steric demand, and it neither interacts with nor labels ds17, as further confirmed by a poststaining step with an undiscriminating DNA labeling probe (SYBR Safe, Figure 5B). PyroTASQ is thus a very promising molecular tool in detecting quadruplexes in an efficient and highly specific manner.

■ CONCLUSIONS

On the basis of an unprecedented strategy that harnesses photophysical properties that have long been known but seldom combined in a single molecular scaffold, we have

dx.doi.org/10.1021/ja506331x | J. Am. Chem. Soc. 2014, 136, 12406−12414

converted the first prototype of smart quadruplex ligand into the first prototype of twice-as-smart quadruplex ligand: herein, the pyrene template-assembled synthetic G-quartet, aka PyroTASQ, has proven to be both a smart ligand (demonstrated by FRET-melting and NMR investigations) and a smart probe (fluorescence and PAGE analyses). Gained insights into the actual mechanistic origins (NMR and CD studies) that underlie the turn on/turn off fluorescence of PyroTASQ make it a quite unique probe: it operates through a quadruplex-promoted conformational switch that assembles its four guanines into an intramolecular G-quartet (smart ligand), which releases the fluorescence of its pyrene template by diverting the guanine electrons from an electronic restraint that maintains its fluorescence at a lowest level (smart probe). This study thus provides another valuable impetus for multifaceted synthetic G-quartets (TASQ) to be considered as key players for future biotechnological developments, especially in light of their capability to interact with quadruplexes whatever their nature (DNA, RNA) and the sequence they fold from (telomere, promoters region of oncogenes). This ability could represent a significant advantage to determine whether, when, and where quadruplex structures form during the cell cycle, notably in cancer cell lines in which multiple quadruplex-involving pathways are deregulated.

EXPERIMENTAL SECTION

The key procedures are outlined in the following section; full experimental details for the synthesis of PyroTASQ, including syntheses, purifications, and characterizations, are given in the Supporting Information as well as protocols for the preparation of the oligonucleotides.

FRET-Melting Experiments. Experiments were performed in a 96-well format using a Mx3005P qPCR machine (Agilent) equipped with a FAM filter (λ_{ex} = 492 nm; λ_{em} = 516 nm). Dose−response experiments were carried out in 100 μL (final volume) of 10 mM lithium cacodylate buffer (pH 7.2) + 99 mM LiCl/1 mM KCl (except for F21T and F-duplex-T: 90 mM LiCl/10 mM KCl), with 0.2 μM of labeled DNA (F21T (28 μM, 0.7 μL), F-kit-T (31 μM, 0.6 μL), F-myc-T (28 μM, 0.7 μL), and F-duplex-T (36 μM, 0.5 μL)) or RNA oligonucleotides (L-TERRA (18 μM, 1.1 μL), L-VEGF (21 μM, 0.9 μL), and L-TRF2 (23 μM, 0.8 μL)) with increasing amounts (0−25 mol equiv) of PyroTASQ (0−5 μM, 100 μM in H_2O, 0−5 μL). Competitive FRET-melting experiments were carried out in 100 μL (final volume) of 10 mM lithium cacodylate buffer (pH 7.2) + 90 mM LiCl/10 mM KCl (F21T) or 99 mM LiCl/1 mM KCl (L-TERRA), with labeled quadruplex-DNA (F21T, 0.2 μM, 28 μM, 0.7 μL) or quadruplex-RNA (L-TERRA, 0.2 μM, 18 μM, 1.1 μL), in the presence of PyroTASQ (1.0 μM, 100 μM, 1 μL) and increasing amounts (0, 15, and 50 mol equiv) of unlabeled competitors (ds26 (205 μM, 1.4 and 4.9 μL), TG5T (166 μM, 1.8 and 6.1 μL) or UG5U (114 μM, 2.6 and 8.8 μL)). After a first equilibration step (25 °C, 30s), a stepwise increase of 1 °C every 30 s for 65 cycles to reach 90 °C was performed, and measurements were made after each cycle. Final data were analyzed with Excel (Microsoft Corp.) and OriginPro8 (OriginLab Corp.). The emission of FAM was normalized (0−1), and $T_{1/2}$ was defined as the temperature for which the normalized emission is 0.5; $\Delta T_{1/2}$ values are means of 2−4 experiments.

NMR Investigations. ^{1}H NMR spectra were acquired on a Bruker Avance II 600 MHz spectrometer using the "1D_watergate" solvent suppression sequence (p3919gp pulse sequence). The quadruplex forming DNA sequence $[T_2AG_3T]_4$ was prepared by dissolving lyophilized T_2AG_3T strands (468.0 nmol) in 600 μL of 10 mM lithium cacodylate buffer (pH 7.2) + 90 mM LiCl/10 mM KCl and folded by heating (90 °C, 15 min), progressively cooling (70 °C (30 min) then 65, 60, 55, 50, 40, and 30 °C (60 min each step), 25 °C (2 h)) and then stored overnight (4 °C). The actual concentration, determined by dilution to 0.50 μM theoretical motif concentration and UV−vis spectral analysis at 260 nm (after 5 min at 90 °C) with the molar extinction coefficient value provided by the manufacturer (ε = 279200 L·mol^{-1}·cm^{-1}), was 249 μM. The ^{1}H NMR spectra of PyroTASQ alone and DNA alone (650 μL, prepared by mixing $[T_2AG_3T]_4$ (249 μM, 540 μL) with D_2O (60 μL) to obtain a 224 μM final DNA concentration) was recorded after 20000 scans. Subsequent experiments were realized after additions of 5 × 0.2 mol equiv of PyroTASQ (10 mM in water, 5 × 2.7 μL) and 18000 scans.

Fluorescence Investigations. Spectra were recorded on a JASCO FP8500 spectrofluorometer in a 10 mm path-length semimicro quartz cuvette (Starna). All experiments were carried out in 1 mL (final volume) of 10 mM lithium cacodylate buffer (pH 7.2) + 90 mM LiCl/10 mM KCl, with PyroTASQ (2 μM, 10 mM in H_2O, 0.2 μL) alone or in the presence of DNA/RNA oligonucleotides (4 μM) being either duplexes (ds17 (153 μM, 26.1 μL), ds26 (205 μM, 19.5 μL), and CT-DNA (3.1 mM, 2.6 μL)) or quadruplexes (22AG (336 μM, 11.9 μL), c-kit (323 μM, 12.4 μL), c-myc (317 μM, 12.6 μL), TERRA (275 μM, 14.5 μL), and SRC (305 μM, 13.1 μL)). Spectra (λ_{ex} = 420 nm, λ_{em} = 435−700 nm, Ex and Em slits = 5 nm, 1 nm pitch, 2 s response, scan speed = 500 nm·min^{-1}) were recorded 15 min (at 25 °C) after the addition of the oligonucleotide. Competitive fluorescence experiments were carried out in 1 mL (final volume) of 10 mM lithium cacodylate buffer (pH 7.2) + 90 mM LiCl/10 mM KCl, with PyroTASQ (2 μM, 10 mM in H_2O, 0.2 μL) plus SRC (4 μM, 305 μM, 13.1 μL) and increasing amounts of CT-DNA (2−200 μM, 3.1 mM, 0.6−64.0 μL)). Final data were analyzed with OriginPro8 (OriginLab Corp.).

CD and UV−vis Spectroscopy. CD spectra were recorded on a JASCO J-815 spectropolarimeter and UV−vis spectra on a JASCO V630Bio spectrophotometer in a 10 mm path-length quartz semimicro cuvette (Starna). CD spectra were recorded over a range of 220−500 nm (bandwidth = 0.5 nm, 1 nm pitch, 1 s response, scan speed = 500 nm·min^{-1}, averaged over 3 scans, zeroed at 500 nm) with PyroTASQ alone (30 μM, 10 mM in H_2O, 3.0 μL) in 1 mL (final volume) of 10 mM lithium cacodylate buffer (pH 7.2) + 90 mM LiCl/10 mM KCl or 100 mM KCl. UV−vis experiment was carried out with PyroTASQ alone (10 μM, 10 mM in H_2O, 1.0 μL) in 1 mL (final volume) of 10 mM lithium cacodylate buffer (pH 7.2) + 90 mM LiCl/10 mM KCl. CD spectra of quadruplexes (2 μM) were recorded over a range of 220−700 nm (bandwidth = 0.5 nm, 1 nm pitch, 1 s response, scan speed = 500 nm·min^{-1}, averaged over 3 scans, zeroed at 700 nm) with c-myc (484 μM, 4.1 μL) or 22AG (309 μM, 6.5 μL), alone or in the presence of PyroTASQ (4 μM, 2 mM in H_2O, 2.0 μL), before or after a thermal annealing step (90 °C for 5 min and quick cooling to 25 °C), in 10 mM lithium cacodylate buffer (pH 7.2) + 90 mM LiCl/10 mM KCl, 50% CH_3CN. Final data were analyzed with OriginPro8 (OriginLab Corp.).

Gel Electrophoresis. Nondenaturing PAGE was carried out with 6% polyacrylamide-bisacrylamide (29:1) gel. Samples were prepared in 10 μL (final volume) of 20 mM lithium cacodylate buffer (pH 7.2) + 150 mM KCl, with DNA (150 μM), i.e., ds17 (294 μM, 5.1 μL), c-myc (320 μM, 4.7 μL), or 22AG (305 μM, 4.9 μL) and increasing amounts (0−2 mol equiv) of PyroTASQ (0−300 μM, 2 mM in H_2O, 0−1.5 μL). The quadruplex-containing samples were heated at 90 °C for 5 min and cooled to room temperature. Loading samples were prepared mixing 2.5 μL of the previously prepared DNA samples (±PyroTASQ) and 5.0 μL of sucrose (15% in H_2O), thus corresponding to a final DNA concentration of 50 μM; 5.0 μL of this mixture was thus loaded on the gel. The electrophoretic migration were performed in 1 × TBE (tris-borate-ethylenediamine tetraacetic acid), pH 8.3 plus 50 mM KCl, for 2 h at 4 °C (50 V). After the migration, gels were analyzed either before or after a post-staining step (SYBR Safe solution, 1:10000, 10 min, 25 °C under gentle agitation) with a UVP MultiDoc-It imaging system (λ_{ex} = 254 nm).

ASSOCIATED CONTENT

Supporting Information

All experimental details and supplementary figures. This material is available free of charge via the Internet at http://pubs.acs.org.

AUTHOR INFORMATION

Corresponding Author

david.monchaud@u-bourgogne.fr

Notes

The authors declare no competing financial interest.

ACKNOWLEDGMENTS

This work was supported by the Centre National de la Recherche Scientifique (CNRS), Université de Bourgogne (uB), Conseil Régional de Bourgogne (CRB), and the Agence Nationale de la Recherche (ANR) via 3MIM, ANR-10-JCJC-0709, and PARI-SSTIC 6 (92-01, CRB) projects. J. Gervais is acknowledged for preliminary FRET-melting investigations and R. Desbourbes and G. Berrez for their assistance with chemical synthesis. The Ministère de l'Enseignement Supérieur et de la Recherche is acknowledged for Ph.D. grants to A.L. and L.S.

REFERENCES

(1) Collie, G. W.; Parkinson, G. N. *Chem. Soc. Rev.* **2011**, *40*, 5867.
(2) Bochman, M. L.; Paeschke, K.; Zakian, V. A. *Nat. Rev. Genet.* **2012**, *13*, 770.
(3) Rodriguez, R.; Miller, K. M.; Forment, J. V.; Bradshaw, C. R.; Nikan, M.; Britton, S.; Oelschlaegel, T.; Xhemalce, B.; Balasubramanian, S.; Jackson, S. P. *Nat. Chem. Biol.* **2012**, *8*, 301.
(4) Jackson, S. P.; Bartek, J. *Nature* **2009**, *461*, 1071.
(5) Martin, S. A.; Lord, C. J.; Ashworth, A. *Curr. Opin. Genet. Dev.* **2008**, *18*, 80.
(6) (a) Salvati, E.; Scarsella, M.; Porru, M.; Rizzo, A.; Iachettini, S.; Tentori, L.; Graziani, G.; D'Incalci, M.; Stevens, M. F. G.; Orlandi, A.; Passeri, D.; Gilson, E.; Zupi, G.; Leonetti, C.; Biroccio, A. *Oncogene* **2010**, *29*, 6280. (b) McLuckie, K. I. E.; Di Antonio, M.; Zecchini, H.; Xian, J.; Caldas, C.; Krippendorff, B.-F.; Tannahill, D.; Lowe, C.; Balasubramanian, S. *J. Am. Chem. Soc.* **2013**, *135*, 9640.
(7) Hurley, L. H. *Nat. Rev. Cancer* **2002**, *2*, 188.
(8) Koirala, D.; Dhakal, S.; Ashbridge, B.; Sannohe, Y.; Rodriguez, R.; Sugiyama, H.; Balasubramanian, S.; Mao, H. *Nat. Chem.* **2011**, *3*, 782.
(9) Ohnmacht, S. A.; Neidle, S. *Bioorg. Med. Chem. Lett.* **2014**, *24*, 2602.
(10) Maizels, N.; Gray, L. T. *PLoS Genet.* **2013**, *9*, e1003468.
(11) Murat, P.; Balasubramanian, S. *Curr. Opin. Gen. Dev.* **2014**, *25*, 22.
(12) Largy, E.; Granzhan, A.; Hamon, F.; Verga, D.; Teulade-Fichou, M.-P. *Top. Curr. Chem.* **2012**, *330*, 111.
(13) Largy, E.; Hamon, F.; Teulade-Fichou, M.-P. *Anal. Bioanal. Chem.* **2011**, *400*, 3419.
(14) Jin, B.; Zhang, X.; Zheng, W.; Liu, X.; Qi, C.; Wang, F.; Shangguan, D. *Anal. Chem.* **2014**, *86*, 943.
(15) Tseng, T.-Y.; Wang, Z.-F.; Chien, C.-H.; Chang, T.-C. *Nucleic Acids Res.* **2013**, *41*, 10605.
(16) Hong, Y.; Xiong, H.; Lam, J. W. Y.; Haussler, M.; Liu, J.; Yu, Y.; Zhong, Y.; Sung, H. H. Y.; Williams, I. D.; Wong, K. S.; Tang, B. Z. *Chem.—Eur. J.* **2010**, *16*, 1232.
(17) Koeppel, F.; Riou, J.-F.; Laoui, A.; Mailliet, P.; Arimondo, P. B.; Labit, D.; Petitgenet, O.; Hélène, C.; Mergny, J.-L. *Nucleic Acids Res.* **2001**, *29*, 1087.
(18) Sabharwal, N. C.; Savikhin, V.; Turek-Herman, J. R.; Nicoludis, J. M.; Szalai, V. A.; Yatsunyk, L. A. *FEBS J.* **2014**, *281*, 1726.
(19) Wang, P.; Leung, C.-H.; Ma, D.-L.; Yan, S.-C.; Che, C.-M. *Chem.—Eur. J.* **2010**, *16*, 6900.
(20) Gill, M. R.; Garcia-Lara, J.; Foster, S. J.; Smythe, C.; Battaglia, G.; Thomas, J. A. *Nat. Chem.* **2009**, *1*, 662.
(21) Alzeer, J.; Vummidi, B. R.; Roth, P. J. C.; Luedtke, N. W. *Angew. Chem., Int. Ed.* **2009**, *48*, 9362.
(22) Vummidi, B. R.; Alzeer, J.; Luedtke, N. W. *ChemBioChem* **2013**, *14*, 540.
(23) Meguellati, K.; Koripelly, G.; Ladame, S. *Angew. Chem., Int. Ed.* **2010**, *49*, 2738.
(24) Vy Thi Le, T.; Han, S.; Chae, J.; Park, H. J. *Curr. Pharm. Des.* **2012**, *18*, 1948.
(25) Haider, S. M.; Neidle, S.; Parkinson, G. N. *Biochimie* **2011**, *93*, 1239.
(26) Haudecoeur, R.; Stefan, L.; Denat, F.; Monchaud, D. *J. Am. Chem. Soc.* **2013**, *135*, 550.
(27) Nikan, N.; Sherman, J. C. *Angew. Chem., Int. Ed.* **2008**, *47*, 4900.
(28) (a) Stefan, L.; Guédin, A.; Amrane, S.; Smith, N.; Denat, F.; Mergny, J.-L.; Monchaud, D. *Chem. Commun.* **2011**, *47*, 4992. (b) Stefan, L.; Denat, F.; Monchaud, D. *J. Am. Chem. Soc.* **2011**, *133*, 20405.
(29) Haudecoeur, R.; Stefan, L.; Monchaud, D. *Chem.—Eur. J.* **2013**, *19*, 12739.
(30) Ostergaard, M. E.; Hrdlicka, P. J. *Chem. Soc. Rev.* **2011**, *40*, 5771.
(31) Lee, Y. O.; Pradhan, T.; Yoo, S.; Kim, T. H.; Kim, J.; Kim, J. S. *J. Org. Chem.* **2012**, *77*, 11007.
(32) For seminal articles, see: (a) Dieck, H. A.; Heck, F. R. *J. Organomet. Chem.* **1975**, *93*, 259. (b) Cassar, L. *J. Organomet. Chem.* **1975**, *93*, 253. (c) Sonogashira, K.; Tohda, Y.; Hagihara, N. *Tetrahedron Lett.* **1975**, 4467. for an authoritative review, see: Doucet, H.; Hierso, J.-C. *Angew. Chem., Int. Ed.* **2007**, *46*, 834.
(33) de Silva, A. P.; Moody, T. S.; Wright, G. D. *Analyst* **2009**, *134*, 2385.
(34) Renciuk, D.; Zhou, J.; Beaurepaire, L.; Guédin, A.; Bourdoncle, A.; Mergny, J.-L. *Methods* **2012**, *57*, 122.
(35) Xu, Y. *Chem. Soc. Rev.* **2011**, *40*, 2719.
(36) Balasubramanian, S.; Hurley, L. H.; Neidle, S. *Nature Rev. Drug Discovery* **2011**, *10*, 261.
(37) Luke, B.; Lingner, J. *EMBO J.* **2009**, *28*, 2503.
(38) Bugaut, A.; Balasubramanian, S. *Nucleic Acids Res.* **2012**, *40*, 4727.
(39) Lacroix, L.; Séosse, A.; Mergny, J.-L. *Nucleic Acids Res.* **2011**, *39*, e21.
(40) Di Antonio, M.; Biffi, G.; Mariani, A.; Raiber, E.-A.; Rodriguez, R.; Balasubramanian, S. *Angew. Chem., Int. Ed.* **2012**, *51*, 11073.
(41) Gilli, G.; Bellucci, F.; Ferretti, V.; Bertolasi, V. *J. Am. Chem. Soc.* **1989**, *111*, 1023.
(42) Fonseca Guerra, C.; Zijlstra, H.; Paragi, G.; Bickelhaupt, F. M. *Chem.—Eur. J.* **2011**, *17*, 12612.
(43) Karsisotis, A. I.; Hessari, N. M.; Novellino, E.; Spada, G. P.; Randazzo, A.; Webba da Silva, M. *Angew. Chem., Int. Ed.* **2011**, *50*, 10645.
(44) Yang, D.; Okamoto, K. *Future Med. Chem.* **2010**, *2*, 619.
(45) Kato, Y.; Ohyama, T.; Mita, H.; Yamamoto, Y. *J. Am. Chem. Soc.* **2005**, *127*, 9980.
(46) Wang, Y.; Patel, D. J. *Biochemistry* **1992**, *31*, 8112.
(47) Gavathiotis, E.; Heald, R. A.; Stevens, M. F. G.; Searle, M. S. *Angew. Chem., Int. Ed.* **2001**, *40*, 4749.
(48) Bare, G. A.; Liu, B.; Sherman, J. C. *J. Am. Chem. Soc.* **2013**, *135*, 11985.
(49) Buscaglia, R.; Miller, M. C.; Dean, W. D.; Gray, R. D.; Lane, A. L.; Trent, J. O.; Chaires, J. B. *Nucleic Acids Res.* **2013**, *41*, 7934.
(50) Viovy, J.-L. *Rev. Mod. Physics* **2000**, *72*, 813.
(51) Richards, A. D.; Rodger, A. *Chem. Soc. Rev.* **2007**, *36*, 471.
(52) Renaud de la Faverie, A.; Guédin, A.; Bedrat, A.; Yatsunyk, L. A.; Mergny, J.-L. *Nucleic Acids Res.* **2014**, *42*, e65.
(53) Xie, X.; Choi, B.; Largy, E.; Guillot, R.; Granzhan, A.; Teulade-Fichou, M.-P. *Chem.—Eur. J.* **2013**, *19*, 1214.